


Modeling of Hydration, Strength Development, and Optimum Combinations of Cement-Slag-Limestone Ternary Concrete

Xiao-Yong Wang^{1)*} , and Yao Luan²⁾

(Received September 12, 2017, Accepted January 5, 2018)

Abstract: Slag can increase late age strength of concrete, but impairs the concrete early-age strength due to low reactivity. Limestone powder can increase early-age strength, but impairs late-age strength due to dilution effect. The combination of slag and limestone powder can produce a composite concrete with adequate strength at both early ages and late ages. This study shows an integrated hydration-strength-optimization model for cement-slag-limestone ternary blends. First, a blended hydration model is put forward for simulating the hydration of composite binder containing slag and limestone powder. Reaction degrees of individual component of binders are calculated using this hydration model. Second, the gel-space ratio of ternary blended concrete is determined based on reaction degrees of composite binder and mixing proportions. Moreover concrete compressive strength is calculated using gel-space ratio. Third, based on parameters analysis, the isoresponse curves regarding strength of concrete are calculated. The optimum combinations of cement, slag, and limestone powder at different ages are calculated. The proposed numerical procedure is valuable for optimum strength design of cement-slag-limestone ternary concrete.

Keywords: slag, limestone powder, ternary blended concrete, hydration model, optimum combinations.

1. Introduction

Slag and limestone powder are increasingly used in producing high performance concrete. Slag and limestone present different effects on strength development of concrete. Limestone contributes to young age strength of concrete and slag increases long term strength of concrete. When slag and limestone are used together, due to the synergy effect, adequate strength at both young age and long term age can be achieved (Papadakis 2000; Bonavetti et al. 2003).

Many experimental and theoretical studies have been done about cement-slag-limestone ternary blended concrete. Menendez et al. (2003) and Carrasco et al. (2005) measured compressive strength of limestone powder and slag ternary blended concrete with different mixing proportions. They found that whatsoever ages, there's a mix of limestone, slag, and cement that presents the best possible compressive strength, much better than limestone or slag binary blended concrete. Hoshino et al. (2006) found the strength increasing effect of limestone powder is more produced in cement-slag binary system than cement unitary system. This is due to the high aluminum content in slag compositions. Mounanga

et al. (2011) found that ternary binders containing a moderate addition of limestone powder present equal or higher early-age performance compared to concrete containing plain cement. Ghrici et al. (2007) reported that ternary blended concrete exhibits better chloride permeability resistance than plain concrete or binary concrete.

In contrast to abundant experimental studies, theoretical research is relatively limited. Maekawa et al. (2009) analyzed the acceleration of cement hydration due to limestone additions. Moreover, the adiabatic temperature rise of cement-slag-limestone blends was calculated. Gao et al. (2013) simulated the development of microstructure in interfacial transition zone (ITZ) of cement-slag-limestone blended concrete. The anhydrous fraction and porosity in ITZ were calculated. However, Maekawa et al. (2009) and Gao et al. (2013)'s studies do not consider the chemical reaction of limestone powder. Bentz (2006) proposed a model about the dilution, nucleation, and chemical effects of limestone addition. The formation of monocarboaluminate due to limestone reaction was considered (Bentz 2006). However, Bentz's study (2006) mainly focused on limestone binary blended concrete. Antoni et al. (2012) and Lothenbach et al. (2008) made thermodynamic simulations for limestone binary or ternary blended concrete. The phase volume fractions of hydrating concrete were determined using thermodynamic modeling. However, Antoni et al. (2012) and Lothenbach et al. (2008)'s studies mainly focused on the chemical aspect of ternary blended concrete. Regarding the combinations of cement-slag-limestone to obtain optimum compressive strength, current models

¹⁾Department of Architectural Engineering, Kangwon National University, Chuncheon-si, Korea.

*Corresponding Author; E-mail: wxbrave@kangwon.ac.kr

²⁾Department of Civil and Environmental Engineering, Saitama University, Saitama, Japan.

(Maekawa et al. 2009; Gao et al. 2013; Bentz 2006; Antoni et al. 2012; Lothenbach et al. 2008) do not consider this point.

To conquer the problems of current models, this study presents a simulation model which can determine the optimum combinations of cement, slag, and limestone. This simulation model begins with a ternary blended hydration model. The gel-space ratio and compressive strength ratio are determined from reaction degrees of binders. The optimum combinations of cement, slag, and limestone are determined based on parameters analysis.

2. Simulation of Hydration of Cement-Slag-Limestone Ternary Blends

2.1 Simulation of Hydration of Cement-Slag Binary Blends

Our previous study (Lee and Wang 2016) presented a kinetic cement-slag blends hydration model. This kinetic hydration model includes three sub-models, i.e. model for hydration of cement, model for reaction of slag, and model for mutual effects between hydration of cement and reaction of slag. Model for hydration of cement views the kinetic stages involved with hydration of cement, for example initial dormant stage, chemical-reaction related stage, and diffusion related stage. The model of cement hydration also views water withdrawal because of the insufficient capillary water regarding high strength concrete. The equation of cement hydration is simplified written as follows (Lee and Wang 2016):

$$\frac{d\alpha}{dt} = f(k_d(T), D_e(T), k_r(T), r_0) * C_{w-free} * (S_w/S_0) \quad (1)$$

where α is degree of hydration, t is time, $\frac{d\alpha}{dt}$ is rate of hydration of cement, k_d is rate of coefficient in initial dormant stage, T is curing temperature, k_r is rate of coefficient in reaction controlled process, D_e is rate of coefficient in diffusion controlled process, r_0 is the unreacted cement particle radius, S_w means the effective contact area between the surrounding capillary water and cement particles (Lee and Wang 2016), S_0 means the total area if cement hydration products progress unconstrained, C_{w-free} is capillary water content ($C_{w-free} = \left(\frac{W_0 - 0.4C_0\alpha}{W_0}\right)^r$ where C_0 is cement content in concrete mixing proportions, W_0 is the content of water in the proportions of concrete mix, r ($r = 2.6 - 4\frac{W_0}{C_0}$) is an empirical factor considering the approachability of capillary water from outer hard shell to inner anhydrous part of cement particles).

The rate coefficients k_d , k_r , and D_e can be determined based on compound compositions of cement (Lee and Wang 2016). The effect of temperature on rate of hydration of cement is recognized as through Arrhenius's law (Lee and Wang 2016). For high strength concrete, degree of hydration is reduced due to the withdrawal of capillary water. The water withdrawal mechanism is considered through (S_w/S_0) and C_{w-free} in Eq. (1). (S_w/S_0) describes the decrease in contact area between cement particle and ambient capillary water, and C_{w-free} describes the decrease in capillary water concentration.

Similar with hydration of cement, reaction of slag also includes three stages, initial dormant stage, chemical-reaction related stage, and diffusion related stage. Additionally, reaction of slag relies upon calcium hydroxide content in cement-slag blends. The equation of slag reaction is simplified written as follows (Lee and Wang 2016):

$$\frac{d\alpha_{SG}}{dt} = f(k_{dSG}(T), D_{eSG}(T), k_{rSG}(T), r_{SG_0}) * \frac{m_{CH}(t)}{P} \quad (2)$$

where α_{SG} is reaction degree of slag, $\frac{d\alpha_{SG}}{dt}$ is rate of reaction of slag, k_{dSG} is rate of coefficient in initial dormant period of slag, D_{eSG} is rate of coefficient in diffusion controlled process of slag, k_{rSG} is rate of coefficient in reaction controlled process of slag, r_{SG_0} is unreacted slag particle radius, $m_{CH}(t)$ is the calcium hydroxide (CH) content in cement-slag blends, P is slag content in proportions of concrete mixing.

The reaction degrees of cement and slag can be calculated using model of hydration of cement-slag blends. In addition, the thermal qualities, mechanical qualities, and durability of slag blended concrete can be determined using reaction degree of individual component of binders. The cement-slag binary hydration model is multiply validated using experimental results for concrete with various proportions mixes. However, because the cement-slag binary hydration model does not consider the effect of limestone, binary hydration model can not be employed to analyze the hydration of cement-slag-limestone ternary concrete.

2.2 Limestone Powder Reaction Model

Bentz (2006) reported that the addition of limestone presents dilution, nucleation, and chemical effects on hydration of cement. Dilution effect happens when limestone substitutes partial cement, cement content decreases and water to cement ratio increases correspondingly. Nucleation effect is the fact that limestone may work as nucleation sites of hydrating cement. Hydration of cement can accelerate due to nucleation effect. Chemical effect is the formation of monocarboaluminate due to limestone reaction in preference to a monosulfoaluminate.

Similar to slag blended concrete, the dilution effect of limestone powder can be considered by $\frac{C_0}{W_0}$ term in Eq. (1). Regarding nucleation effect, Wang (2017) proposed that the nucleation effect of limestone relates to the ratio of surface area of cement particles to that of limestone powder. The nucleation effect indicator of limestone powder can be written as follows (Wang 2017):

$$L_r = \frac{LS_0 * S_{LS}}{C_0 * S_C} \quad (3)$$

where L_r denotes the indicator of nucleation effect from limestone addition, LS_0 denotes the limestone mass in proportions of concrete mix, S_{LS} denotes the specific surface (Blaine) of limestone, and S_C denotes the specific surface (Blaine) of cement. Maekawa et al. (2009) reported that nucleation effect of limestone is significant in reaction related stage and diffusion related stage. Based on the experimental results of degree of hydration of cement in

cement-limestone blends, Wang (2017) proposed that the nucleation effect of limestone powder can be described as follows:

$$k_{rLS} = k_r(1 + 1.2L_r) \quad (4)$$

$$D_{eLS} = D_e(1 + 1.2L_r) \quad (5)$$

where k_{rLS} is the updated phase boundary reaction coefficient in cement-limestone blends, 1.2 is enhance coefficients of k_r (Wang 2017), D_{eLS} is the updated diffusion coefficient in cement-limestone blends, and 1.2 is enhance coefficients of D_e (Wang 2017).

Ipavec et al. (2011) measured carboaluminate phases formation during hydration of limestone powder blended paste (the water to binder ratio is 0.5, the limestone replacement ratio is 0.2, and curing temperature is 20 °C). The contents of carboaluminate phases were measured at 1, 3, 7, 15, 28, and 100 days monocarboaluminate is main hydration products of limestone at late ages. Based on monocarboaluminate contents, we suggested that the degree of reaction of limestone powder can be calculated as below:

$$\alpha_{LS1} = 0.0087 \ln(t) - 0.0265 \quad (t > 21) \quad (6)$$

where α_{LS1} is the reaction degree of limestone powder, and t is age(hours). The evaluation results about reaction degree of limestone are shown in Fig. 1. Figure 1 shows that reaction degree of limestone is a logarithm function of time, which is similar to the relation between hydration degree of cement and curing age (Lee and Wang 2016). Figure 1 also shows that the reaction of limestone starts after about 21 h, not immediately after mixing. Bentz (2006) also proposed that limestone reaction starts only when the initial calcium sulfate is fully consumed and the formed ettringite phase begins to convert to the AFm phase. Lothenbach (2008) reported that after about 1 day, the reaction of limestone starts. The starting time of limestone in Lothenbach et al. (2008)'s study (1 day) is similar with our study (21 h). In addition, by using Eq. (6), we can found that at the age of

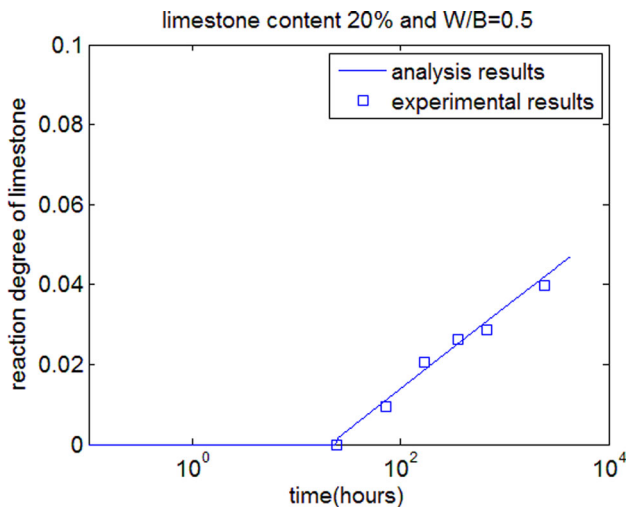


Fig. 1 Reaction degree of limestone.

180 days, the reaction degree of limestone is about 4.6%, which is similar to the results of Bentz's study (Bentz 2006) proposed that for concrete with 20% limestone, at the age of 180 days, about 5% limestone reacted). The reactivity of limestone is much lower than cement or slag.

On the other hand, we should notice that Eq. (6) is only valid for Ipavec et al. (2011)'s study (water to binder ratio was 0.5, limestone replacement ratio was 0.2, and curing temperature was 20 °C). Limestone reaction is a complex process and relates to abundant factors. The factors, such as limestone replacement ratios, slag addition, limestone fineness, cement fineness, water to binder ratio, and curing temperature, will affect the limestone reaction. Considering these points, we propose a more general equation for determined reaction degree of limestone as follows:

$$\alpha_{LS} = \alpha_{LS1} * m_1 * m_2 * m_3 * m_4 * m_5 * m_6 \quad (7)$$

where m_1 considers the effect of limestone replacement ratios on reaction degree of limestone, m_2 considers the effect of limestone fineness, m_3 considers the effect of cement fineness, m_4 considers the effect of slag addition, m_5 considers the effect of water to binder ratio, and m_6 considers the effect of curing temperature.

2.2.1 Effect of Limestone Replacement Ratios

Antoni et al. (2012) reported that as limestone replacement level increases, the reaction degree of limestone powder decreases. This trend is similar with the reaction degree of slag in cement-slag composite concrete (Lee and Wang 2016). Based on Antoni et al. (2012)'s results, we found that the reaction degree of limestone is approximately an inverse proportional function of limestone replacement ratio (shown in Fig. 2a). Hence we assume that $m_1 = \frac{0.2}{\frac{L_{S0}}{C_0 + L_{S0}}}$ (when limestone replacement ratio is 0.2, $m_1 = 1$ which is the case of Ipavec et al. (2011)'s study).

2.2.2 Fineness of Limestone

Aqel and Panesar (2016) reported that when average particle size of limestone powder decreases, the reactivity of limestone increases. Based on Aqel and Panesar's (2016) study about the relation between reaction degree and particle size of limestone (shown in Fig. 2b), we assumed that $m_2 = 1.0131 - 0.0144 * d_{LS}$ where d_{LS} is average diameter of limestone ($m_2 = 1$ is the case of Ipavec et al. (2011)'s study).

2.2.3 Fineness of Cement

Aqel and Panesar (2016) found that when the Blaine surface of cement increases, the average reaction degree of limestone also increases. Based on Aqel and Panesar (2016)'s study, we assumed that $m_3 = 0.55 \frac{S_C}{S_{C1}} + 0.45$ (shown in Fig. 2c) where S_{C1} is the Blaine surface of cement used in Ipavec et al. (2011)'s study (when $S_C = S_{C1}$, $m_3 = 1$ is the case of Ipavec et al. (2011)'s study).

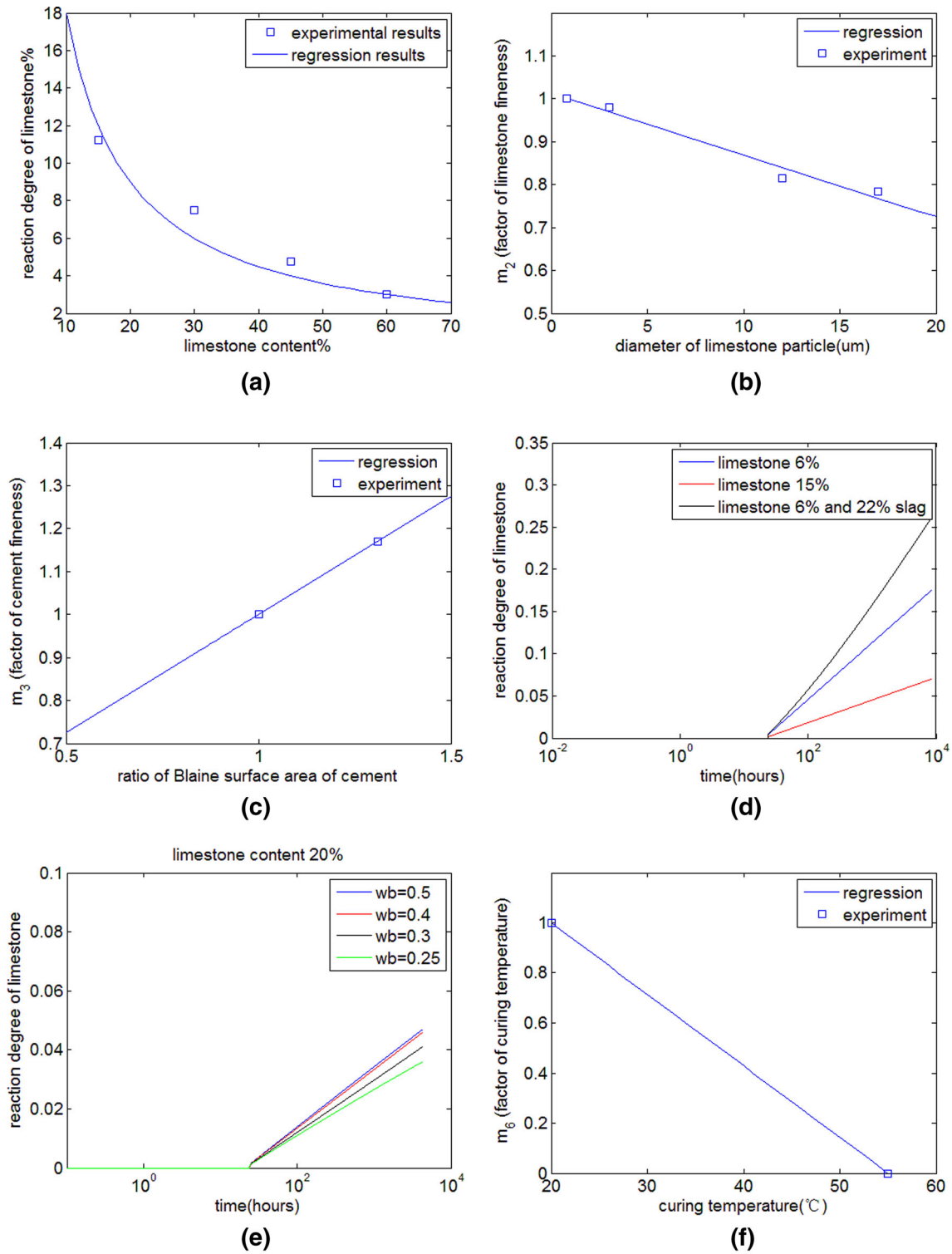


Fig. 2 Modification factors of limestone reaction. **a** limestone replacement ratios, **b** finenes of limestone, **c** fineness of cement, **d** slag additions: water to binder ratio 0.5, **e** water to binder ratios: 20% limestone, **f** curing temperature.

2.2.4 Slag Additions

Hoshino et al. (2006) reported that due to the high aluminum content in slag, the limestone reaction in cement-slag-limestone ternary blends is enhanced. We suggested that the influence of slag on limestone addition can be described as $m_4 = 1 + \frac{Al_{SG}\alpha_{SG}P}{Al_C\alpha_C}$, where Al_{SG} is aluminum content in slag, Al_C is aluminum content in cement, $Al_{SG}\alpha_{SG}P$ in numerator is reacted aluminum content from slag reaction, and $Al_C\alpha_C$ in denominator is reacted aluminum content from cement

reaction). As shown in Fig. 2d, slag additions increase reaction degree of limestone. For plain Portland cement, $m_4 = 1$ which is the case of Ipavec et al. (2011)'s study.

2.2.5 Water to Binder Ratios

Similar with cement hydration, the reaction products of limestone deposits in the pore space of concrete. We assumed that as water to binder ratio increases, reaction degree of limestone increases consequently (shown in

Fig. 2e). We proposed that $m_5 = \frac{\alpha}{\alpha_{0.5}}$ where $\alpha_{0.5}$ is reaction degree of cement for the case of water to binder ratio 0.5. When water to binder ratio equals to 0.5, $m_5 = 1$ which is the case of Ipavec et al. (2011)'s study.

2.2.6 Curing Temperature

Aqel and Panesar (2016) proposed that when curing temperature increases, due to the decreasing of solubility of limestone, the chemical reaction of limestone is reduced. Based on Aqel and Panesar (2016)'s experimental study, we assumed that when curing temperature is higher than 55 °C, the limestone reaction ceases. Hence $m_6 = 1 - \frac{T-20}{35}$ (shown in Fig. 2f). When curing temperature is 20 °C, $m_6 = 1$ which is the case of Ipavec et al. (2011)'s study.

Summarily, our proposed model considers the dilution, nucleation, and chemical effects of limestone additions. We consider dilution effect by means of concentration of capillary water ($\frac{C_0}{W_0}$ term in Eq. 1). We consider nucleation effect by means of nucleation effect indicator (Eq. 3). Chemical effect is considered using a logarithm function and multiple modification factors (Eqs. 6 and 7). The modification factors reflect the general trends of reaction degree of limestone powder. However, because the available experimental results about reaction degree of limestone are very limit, the calibrations of modification factors still need further study. Other influencing factors, such as the aluminum and gypsum content in cement, also need more study.

2.3 Interactions Among Reactions of Cement, Slag, and Limestone

In this study, the contents of calcium hydroxide (CH) and capillary water in hydrating cement-slag-limestone blends are adopted as fundamental indicators to consider mutual effects among the reactions of cement, slag, and limestone. Bentz (2006) proposed that when 1 g limestone powder reacts, 1.62 g water will be consumed. The consumed water of limestone powder is much higher than that of cement or slag. This is because the reaction products of limestone powder are monocarboaluminate and ettringite which contains abundant water. For cement-slag-limestone ternary blends, the amount of capillary water W_{cap} can be determined as below:

$$W_{cap} = W_0 - 0.4 * C_0 * \alpha - 0.45 * \alpha_{SG} * P - 1.62 * LS_0 * \alpha_{LS} \quad (8)$$

where $0.4 * C_0 * \alpha$, $0.45 * \alpha_{SG} * P$, and $1.62 * LS_0 * \alpha_{LS}$ are the consumed water from cement hydration, slag reaction, and limestone reaction respectively.

Cement hydration, slag reaction, and limestone reaction will contribute to the formation of chemically bound water. The chemically bound water W_{cbm} can be determined as follows:

$$W_{cbm} = v * C_0 * \alpha + 0.3 * P * \alpha_{SG} + 1.62 * LS_0 * \alpha_{LS} \quad (9)$$

where $v * C_0 * \alpha$, $0.3 * P * \alpha_{SG}$, and $1.62 * LS_0 * \alpha_{LS}$ are the amount of produced chemically bound water produced from

cement hydration, slag reaction, and limestone reaction respectively.

Weerd et al. (2011) measured calcium hydroxide contents for hydrating cement-limestone blends. They found that the calcium hydroxide content in cement-limestone composite specimen is lower compared to control specimen. The calcium hydroxide is consumed due to the production of hemicarbonates from limestone reaction. Based on experimental results of Weerd et al. (2011), we proposed that when 1 g limestone reacts, 0.35 g calcium hydroxide will be consumed. Figure 3 shows that the analysis results about CH generally conform to experimental data. For cement-slag-limestone ternary blends, CH content can be calculated as below:

$$CH(t) = RCH_{CE} * C_0 * \alpha - v_{SG} * \alpha_{SG} * P - 0.35 * \alpha_{LS} * LS_0 \quad (10)$$

where RCH_{CE} means the mass of CH as 1 unit mass of cement hydrates. $RCH_{CE} * C_0 * \alpha$ is the mass of CH produced from cement hydration. $v_{SG} * \alpha_{SG} * P$ and $0.35 * \alpha_{LS} * LS_0$ are the mass of CH consumed from slag reaction and limestone reaction respectively.

Summarily, from Sects. 2.1–2.3, we put forward a simulation model which simulates the hydration of cement-slag-limestone blends. The interactions among cement hydration, slag reaction, and limestone reaction are taken in account by means of the contents of calcium hydroxide and capillary water. This simulation model considers the dilution effect from slag and limestone additions. The nucleation effect of limestone addition is considered using nucleation effect indicator. The chemical reaction of limestone additions is modeled using a logarithm function with multiple modification factors. The input parameters of this numerical procedure are concrete mixing proportions, physical and chemical properties of binders, and curing conditions. Furthermore, by using kinetic reaction equations, the reaction degrees of composite binder can be determined as curing

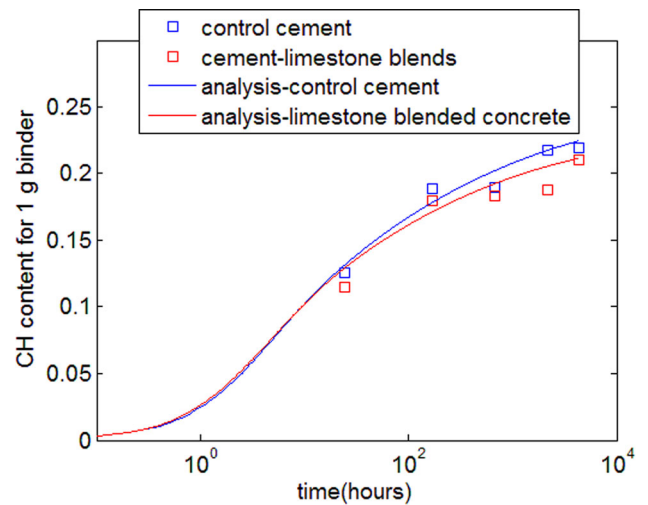


Fig. 3 CH content of cement-limestone blends (water to binder ratio 0.5, 5% limestone).

time progresses. Additionally, it should be noticed that the reaction coefficients of proposed ternary hydration model do not alter for different proportions of concrete mixes. As the combinations of cement, slag, limestone, and water change from one mix to another, the reaction coefficients of ternary hydration model are constant.

2.4 Compressive Strength Development Model

The reaction products of cement hydration, slag reaction, and limestone powder reaction will fill the pore space of concrete. Concrete compressive strength will development with the progress of binders reaction. According to Powers' strength theory, concrete compressive strength can be calculated as below:

$$f_c(t) = Ax_c^n \quad (11)$$

where $f_c(t)$ is concrete compressive strength, A is the intrinsic strength of concrete, x_c is gel-space ratio of concrete, and n is the strength exponent. In addition, it be noticed that Eq. (11) do not consider the influence of aggregate on concrete strength. For normal strength concrete, the influence of aggregate on concrete strength is not significant. The gel-space ratio denotes the volumetric ratio of the hydration products to the sum of hydrated binders and capillary pore. Regarding cement-slag-limestone blends, 2.06 ml space is occupied as 1 ml cement hydrates (Lee and Wang 2016), 2.52 ml space is occupied as 1 ml slag reacts (Lee and Wang 2016), and 4.1 ml space is occupied as 1 ml reacted limestone reacts (Bentz 2006). Reacted products of 1 ml limestone can occupy much higher space than that of cement (4.1 vs. 2.06). This is because of the formation of ettringite and monocarboaluminate from limestone reaction. Considering cement hydration, slag reaction, and limestone reaction, the gel-space ratio of cement-slag-limestone ternary blended cement can be determined as follows:

$$x_c = \frac{2.06(1/\rho_C)\alpha C_0 + 2.52(1/\rho_{SG})\alpha_{SG}P + 4.1(1/\rho_{LS})\alpha_{LS}LS_0}{(1/\rho_C)\alpha C_0 + (1/\rho_{SG})\alpha_{SG}P + (1/\rho_{LS})\alpha_{LS}LS_0 + W_0} \quad (12)$$

where ρ_C , ρ_{SG} , and ρ_{LS} are densities of cement, slag, and limestone powder respectively.

For cement-slag-limestone blends, cement, slag, and limestone will affect the intrinsic strength of concrete and strength exponent. We assume that the intrinsic strength of concrete A and strength exponent n can be written as functions of weight percentages of cement, slag, and limestone in the proportions of concrete mix as follows:

$$A = a1 * \frac{C_0}{C_0 + P + LS_0} + a2 * \frac{P}{C_0 + P + LS_0} + a3 * \frac{LS_0}{C_0 + P + LS_0} \quad (13)$$

$$n = b1 * \frac{C_0}{C_0 + P + LS_0} + b2 * \frac{P}{C_0 + P + LS_0} + b3 * \frac{LS_0}{C_0 + P + LS_0} \quad (14)$$

where coefficients $a1$, $a2$, and $a3$ in Eq. (13) denote the effects of cement, slag, and limestone on the intrinsic strength of concrete, respectively, and the units of $a1$, $a2$, and $a3$ are MPa; the coefficients $b1$, $b2$ and $b3$ in Eq. (14) denote the effects of cement, slag, and limestone on strength exponent, respectively. For neat Portland cement concrete, the weight fractions of limestone and slag are zero, the strength of concrete only relates to $a1$ and $b1$. For slag blended binary concrete, the weight fraction of limestone is zero, and the strength of concrete relates to coefficients $a1$, $a2$, $b1$, and $b2$. For ternary composite concrete, concrete strength relates to coefficients $a1$, $a2$, $a3$, $b1$, $b2$, and $b3$. These coefficients $a1$, $a2$, $a3$, $b1$, $b2$, and $b3$ do not change for various proportions of concrete mix.

The flowchart of calculation is shown in Fig. 4. At every time step, the reaction degrees of cement, slag, and limestone powder are calculated by using ternary blended hydration model. The contents of CH, chemically bound water, and capillary water are determined by using reaction degrees of binders. Furthermore, the gel-space ratio of hydrating concrete is determined taking into account the contributions from individual reactions of cement, slag, and limestone. Based on Powers' strength theory, the concrete compressive strength is calculated.

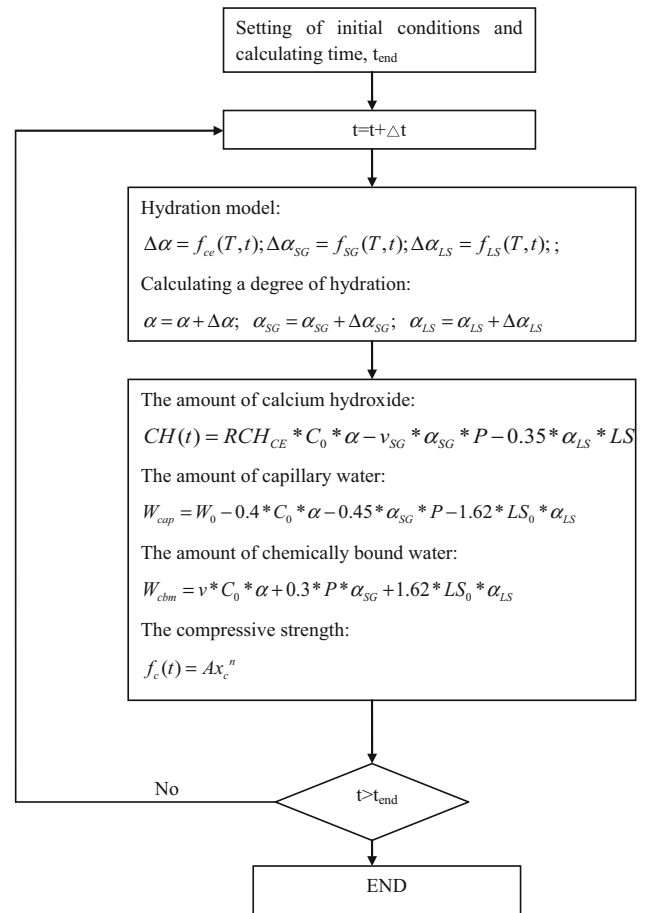


Fig. 4 Flowchart of calculation.

3. Verifications of Proposed Model

3.1 Hydration of Cement-Slag-Limestone Ternary Blends

Experiment data from Hoshino et al. (2006) are adopted to validate the proposed cement-slag-limestone ternary hydration model. Hoshino et al. (2006) made XRD/Rietveld

analysis for hydration of slag and limestone blended cement. The specimens consisted of plain paste (cement paste), binary paste (cement-limestone paste or cement-slag paste), and ternary paste (cement-slag-limestone paste). The reaction degree of cement, calcium hydroxide content, and reaction degree of slag were measured at 3, 7, and 28 days. The water to powder ratio was 0.5, the limestone

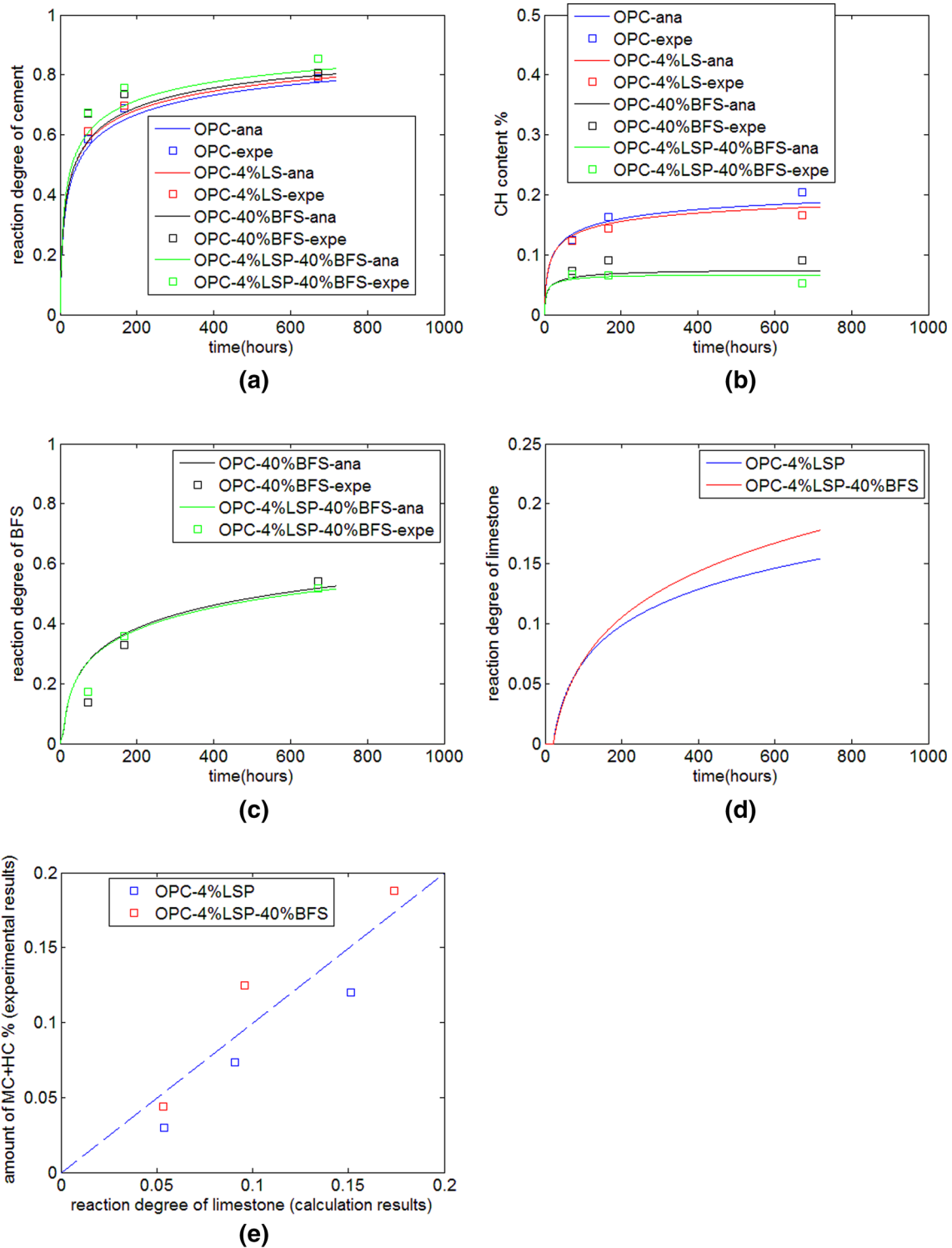


Fig. 5 Properties evaluation of cement-slag-limestone ternary blends. **a** reaction degree of cement, **b** calcium hydroxide content, **c** reaction degree of slag, **d** reaction degree of limestone, **e** relation between reaction degree of limestone and monocarbonate plus hemicarbonate.

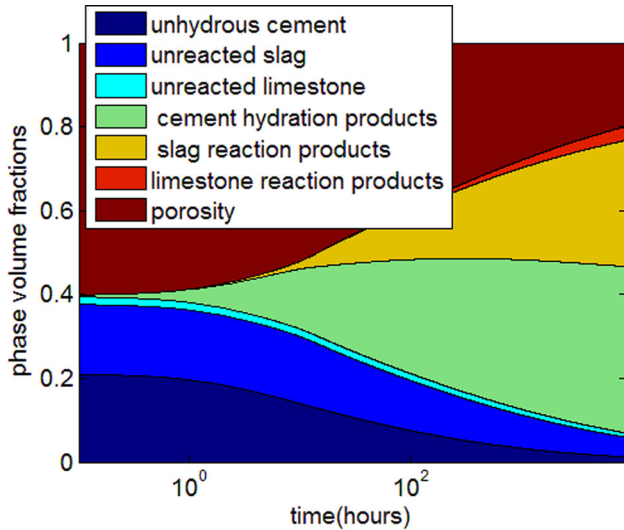


Fig. 6 Phase volume fractions of cement-slag-limestone ternary blends (cement + 4% limestone + 40% slag).

replacement ratio was 4%, slag replacement ratio was 40%, and the curing temperature was 20 °C.

Based on the hydration model of ternary composite cement, the reaction degrees of cement, slag, and limestone powder are determined. Figure 5a shows that the reaction degree of cement for cement-limestone binary paste is higher compared to control paste. This is due to the effects of dilution and nucleation of limestone. The cement-slag-limestone ternary paste has the highest degree of hydration. This is because that the dilution effect from slag, and the nucleation and dilution effect from limestone can accelerate cement hydration. The sequence of degree of hydration is ternary blends > slag blended binary cement > limestone blended binary cement > plain cement. The calculation results from our model can reflect this sequence of degree of cement hydration.

Calcium hydroxide contents can be determined from reaction degree of binders. As shown in Fig. 5b, plain cement has the highest calcium hydroxide (CH) content. On account of the consumption of calcium hydroxide from

limestone reaction and dilution effect of limestone, limestone blended binary cement has a lower CH content than plain cement. The cement-slag-limestone ternary paste has a lowest CH content on account of the consumption of CH from both slag reaction and limestone reaction. The sequence of CH content is plain cement > limestone blended binary cement > slag blended binary cement > ternary paste. The calculation results from our model can reflect this sequence of CH content.

As shown in Fig. 5c, the reaction degree of slag in ternary blended paste is similar to that in cement-slag binary blended paste. First, decreasing of CH content in ternary blended paste will lower the reaction rate of slag. Second, the dilution effect of limestone will increase the capillary water concentration in ternary blends, and increase the reaction rate of slag. Due to the combined actions of increasing factor and decreasing factor, the reaction degree of slag in ternary blended paste is similar with that of binary blended paste. Weerdt et al. (2011) also reported that similar experimental results (the reaction degree of fly ash in cement-fly ash-limestone ternary paste is almost same as that in fly ash blended ternary paste).

Figure 5d shows the reaction degree of limestone in cement-limestone binary blends and cement-slag-limestone ternary blends. Slag addition presents two effects on limestone reaction. First, for cement-limestone blends, as slag replaces partial cement, the ratio of cement to limestone changes (related with factor m_1 of Eq. 7). Second, the aluminum of slag is higher than in cement, which will favor limestone reaction (related with factor m_4 of Eq. 7). At late age, due to the progress of slag reaction, the reaction degree of limestone in ternary paste is higher than that in binary paste.

Hoshino et al. (2006) measured the contents of hemihydrate (Hc) and monohydrate (Mc) at 3, 7, and 28 days. Figure 5e shows the relation between Hc + Mc and reaction degree of limestone for binary paste and ternary paste. Generally, there is a linear relation between reaction products (Hc + Mc) and reaction degree of limestone for different blends.

Table 1 Mixing proportions of mortar specimens (Carrasco et al. 2005).

Mortar	Portland cement (%)	Limestone powder (%)	Blast furnace slag (%)	Water to powder ratio
PC	100	0	0	0.5
C0F6S	94	0	6	0.5
C0F15S	85	0	15	0.5
C6F0S	94	6	0	0.5
C15F0S	85	15	0	0.5
C6F22S	72	6	22	0.5
C11F11S	78	11	11	0.5
C15F22S	63	15	22	0.5
C22F6S	72	22	6	0.5
C22F15S	63	22	15	0.5

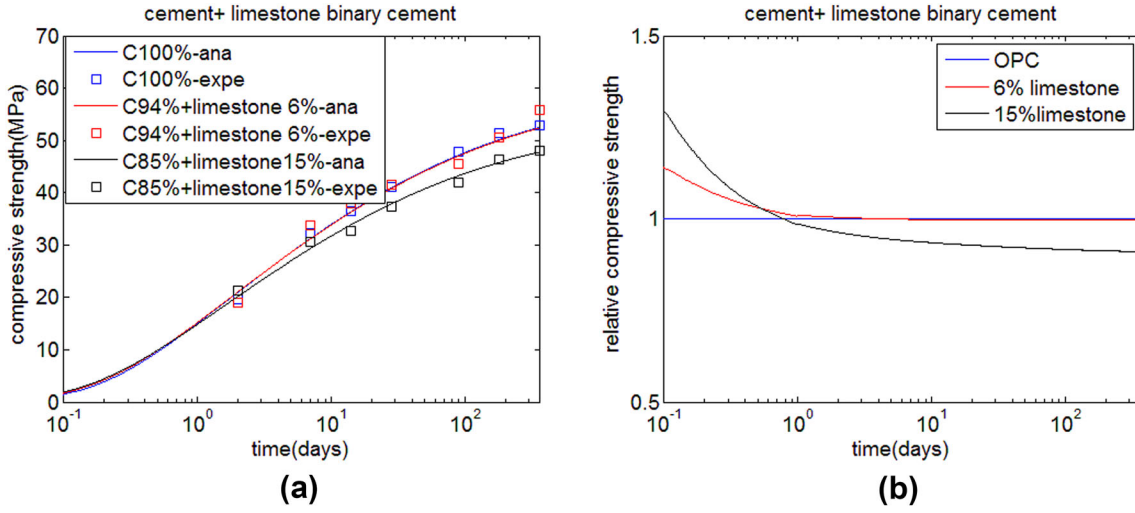


Fig. 7 Strength development of limestone blended concrete. a strength development, b relative strength.

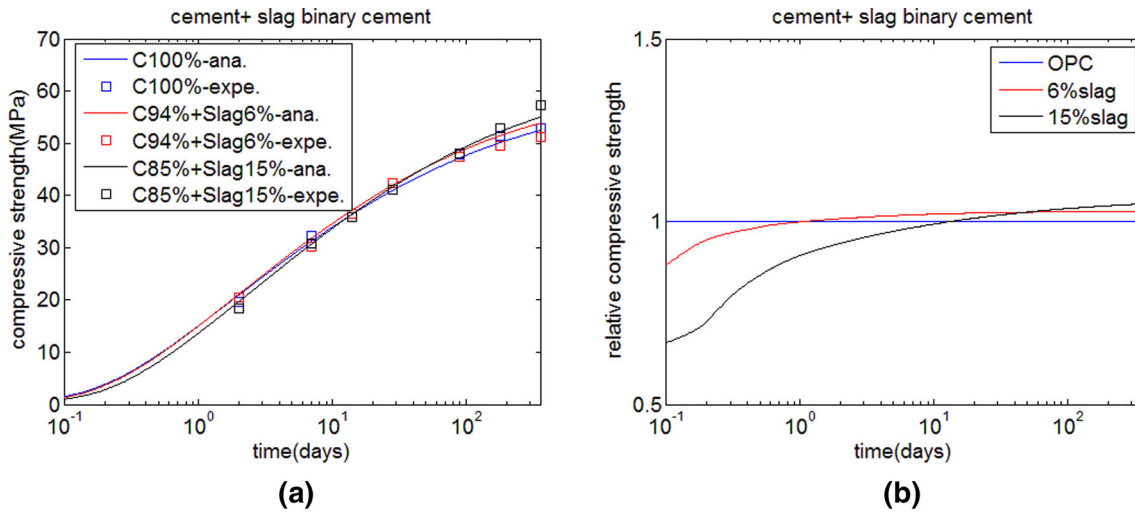


Fig. 8 Strength development of slag blended concrete. a strength development, b relative strength.

Using ternary blended hydration model, volumetric phase fractions of hydrating cement-slag-limestone paste are calculated as below:

$$V_1 = \frac{C_0}{\rho_c} (1 - \alpha) \quad (15)$$

$$V_2 = \frac{P}{\rho_{SG}} (1 - \alpha_{SG}) \quad (16)$$

$$V_3 = \frac{LS_0}{\rho_{LS}} (1 - \alpha_{LS}) \quad (17)$$

$$V_4 = \frac{2.06C_0}{\rho_c} \alpha \quad (18)$$

$$V_5 = \frac{2.52P}{\rho_{SG}} \alpha_{SG} \quad (19)$$

$$V_6 = \frac{4.1LS_0}{\rho_{LS}} \alpha_{LS} \quad (20)$$

$$V_7 = 1 - V_1 - V_2 - V_3 - V_4 - V_5 - V_6 \quad (21)$$

where V_1 , V_2 , V_3 , V_4 , V_5 , V_6 , and V_7 are the volumes of unreacted cement, unreacted slag, unreacted limestone, hydration products of cement, hydration products of slag, hydration products of limestone, and capillary porosity respectively. Figure 6 shows the evolution of volumetric phase fractions of cement-4% limestone-40% slag paste. Because cement hydrates much quicker compared to slag, the remained cement is much less than remained slag. On account of the filling effect of reaction products of binders, the capillary porosity decreases as the evolution of hydration.

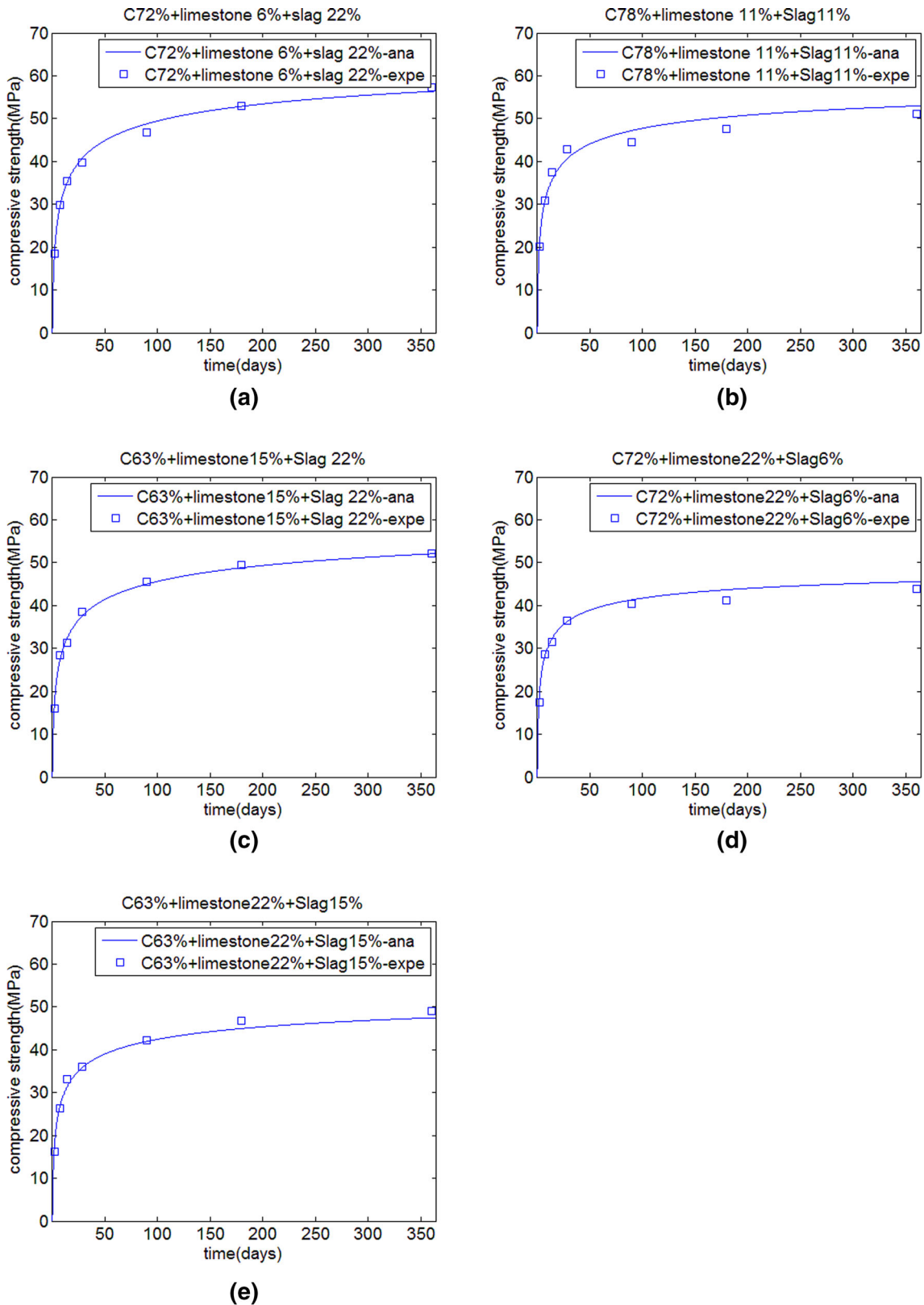


Fig. 9 Strength development of ternary blended paste. **a** 6% limestone +22% slag, **b** 11% limestone + 11% slag, **c** 15% limestone + 22% slag, **d** 22% limestone + 6% slag, **e** 22% limestone + 15% slag.

3.2 Strength Development and Optimal Combinations of Cement-Slag-Limestone Ternary Blends

Based on reaction degrees of individual components in ternary composite, the gel-space ratio can be calculated.

Furthermore, concrete compressive strength can be determined by means of Powers' strength theory. Experimental data from Carrasco et al. (2005) are used to validate the proposed strength development model. Table 1 shows proportions of mortar mix. The water to powder ratio was 0.5,

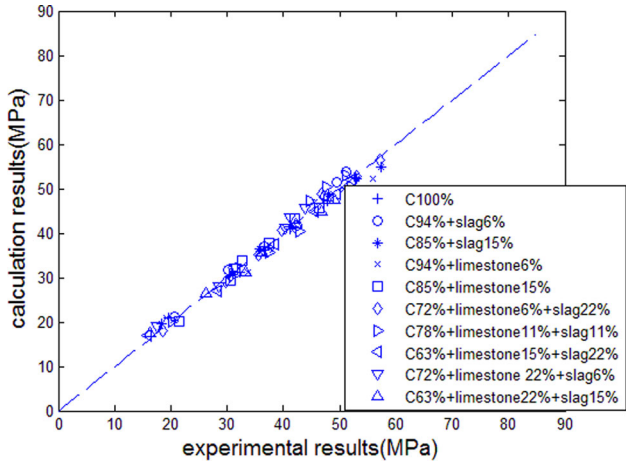


Fig. 10 Comparison between analysis results and experimental results.

and the powder to sand ratio was 1/3. The size of prismatic specimen was $40 \times 40 \times 160 \text{ mm}^3$. One control sample and nine composite samples (binary and ternary) were made. For binary composite specimens the replacement ratios of limestone or slag ranged between 6 and 15%. For ternary composite specimen, the replacement ratios of limestone plus slag ranged between 22 and 37%. The specimens were cured at 20°C . At the ages of 2, 7, 14, 28, 90, 180, and

360 days, the compressive strength of specimen was measured. Total 70 experimental results about compressive strength were obtained (10 mixing proportions \times 7 testing ages = 70).

Using the experimental data of compressive strength, the intrinsic strength coefficients and strength exponents can be calibrated. The values of intrinsic strength coefficients of cement, slag, and limestone are 104.9 MPa (a_1), 151.9 MPa (a_2), and 80.7 MPa (a_3) respectively. The values of strength exponents of cement, slag, and limestone are 2.21 (b_1), 2.60 (b_2), and 2.61 (b_3) respectively. The intrinsic strength coefficients and strength exponents do not change with mixing proportions.

Figure 7a shows the strength development of cement-limestone binary blends and Fig. 7b shows the relative strength of limestone blended concrete (relative strength is the ratio of strength of blended concrete to strength of control concrete). At early ages, limestone additions can increase concrete strength due to acceleration of cement hydration. Concrete containing 15% limestone has a higher strength than concrete containing 6% limestone. While at late ages, due to dilution effect, concrete containing 15% limestone has a lower strength than control concrete. Concrete containing 6% limestone has a similar strength with control concrete.

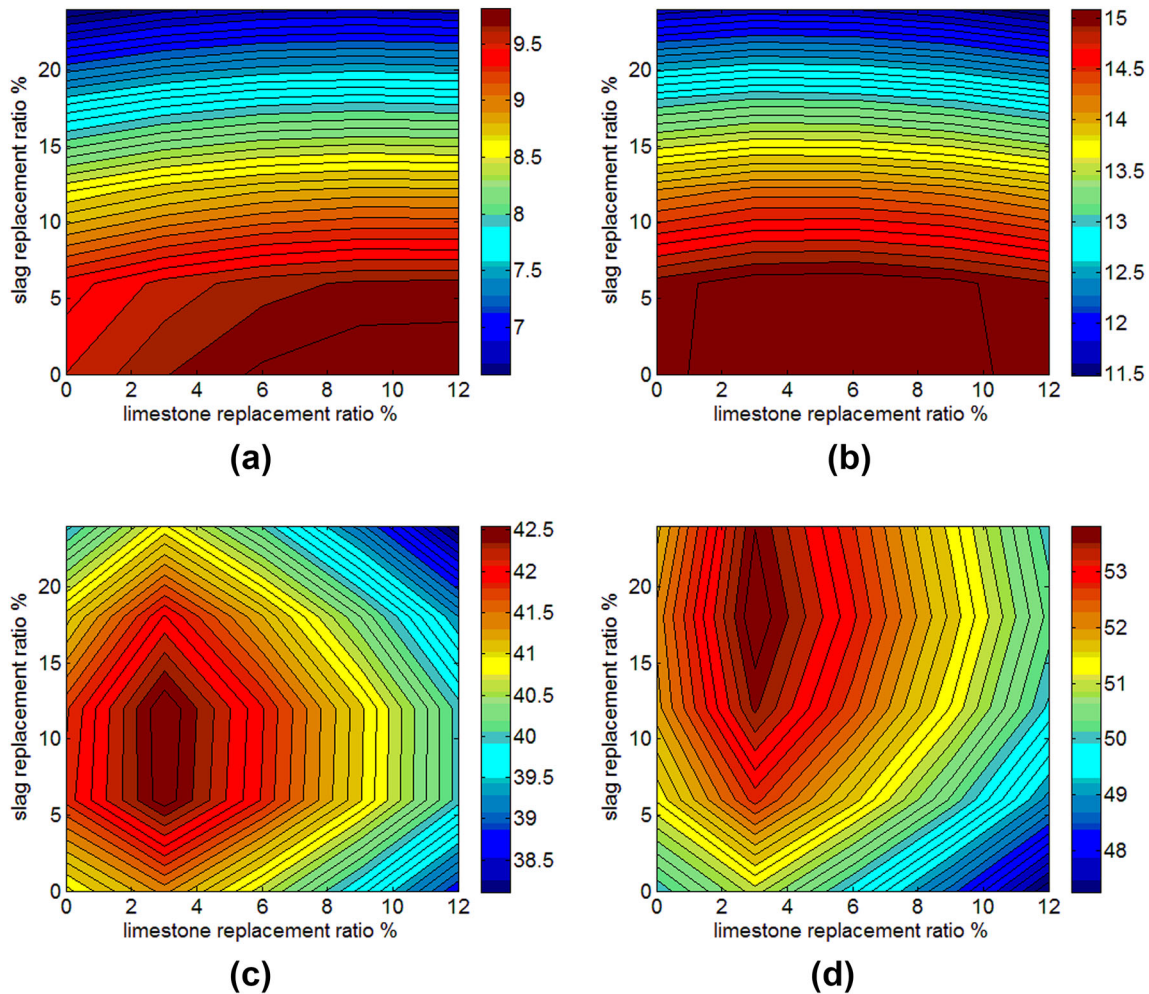


Fig. 11 Isoresponse curve for compressive strength. a 0.5 day, b 1 day, c 28 days, d 180 days.

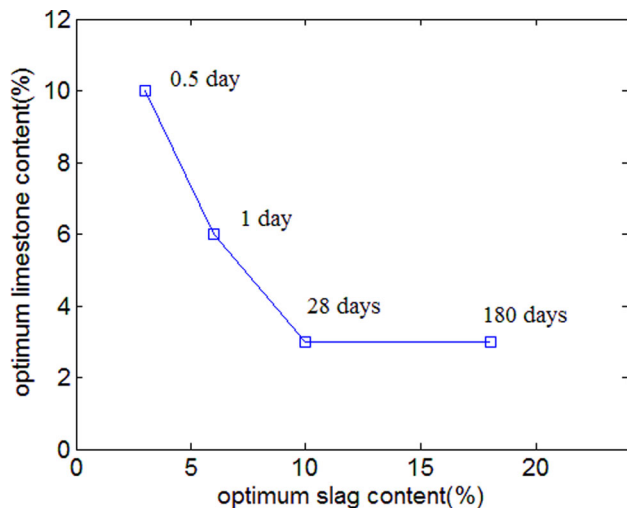


Fig. 12 Optimum percentages of limestone and slag.

Figure 8a shows the strength development of slag blended binary blends and Fig. 8b shows the relative strength of specimens containing different slag contents. Because slag reacts much slower compared to cement, at early-ages, concrete containing slag has lower strength compared to control concrete. With the progress of slag reaction, at late ages, concrete containing slag shows higher strength compared to plain concrete. As slag replacement ratios increases, the reaction degree of slag will decrease (Lee and Wang 2016), and the time corresponding to surpassing strength of control concrete is delayed.

Figure 9 shows the strength development of cement-slag-limestone ternary concrete. The proposed model can evaluate the strength of ternary concrete at both early age (2 days) and late age (360 days). Figure 10 compares analysis results with experimental data. The correlation coefficient between analysis results and experimental data is about 0.99. The root mean square error (RMSE) is about 1.35 MPa. The analysis results generally conform to experimental data.

Limestone powder can improve the young age strength (shown in Fig. 7b) and slag can improve the late-age strength (shown in Fig. 8b). When limestone and slag are used together, the synergy effect can be obtained, and weak points of individual components can be compensated. To find the optimum combinations of cement, slag, and limestone, we make parameter studies about concrete strength development. The slag contents ranges from 0 to 24%, and the limestone contents ranges from 0 to 12%. Figure 11 shows isoresponse curves for compressive strength at different ages (0.5 day, 1 days, 28 days, and 180 days). As shown in Fig. (11a), at early-age 0.5 day, concrete with a higher limestone content and a lower slag content presents a maximum strength. While as shown in Fig. (11d), at late age 180 days, concrete with a higher slag content and a lower limestone content presents a maximum strength.

Figure 12 shows the optimum mixes of slag and limestone regarding highest compressive strength at different ages. From early age to late age, due to the complementary behavior of slag and limestone, the optimum mix shifts from

high limestone-low slag combination to high slag-low limestone combination.

4. Conclusions

This study shows an integrated hydration-strength-optimization model for cement-slag-limestone ternary blends.

First, a blended hydration model is put forward for simulating the hydration of ternary composite binder containing slag and limestone powder. The interactions among cement hydration, slag reaction, and limestone reaction are taken into account by means of the contents of calcium hydroxide and capillary water. The nucleation effect of limestone is considered using nucleation effect indicator, and chemical effect of limestone is modeled using a logarithm function with multiple modification factors. Reaction degrees of binders are calculated using ternary hydration model.

Second, the gel-space ratio of hydrating concrete is determined taking into account the influences of reactions of cement, slag, and limestone. By means of Powers' strength theory, concrete compressive strength is calculated. The strength development model is effective for various ternary blended concrete at different curing ages.

Third, based on parameters analysis, the isoresponse curves for compressive strength are determined. The optimum combinations of cement, slag, and limestone powder at different ages are calculated. From early age to late age, due to the complementary behavior of slag and limestone, the optimum mix shifts from high limestone-low slag combination to high slag-low limestone combination.

Acknowledgements

This research was supported by the Basic Science Research Program through the National Research Foundation of Korea (NRF) funded by the Ministry of Science, ICT & Future Planning (No. 2015R1A5A1037548), and a NRF Grant (NRF-2017R1C1B1010076).

Open Access

This article is distributed under the terms of the Creative Commons Attribution 4.0 International License (<http://creativecommons.org/licenses/by/4.0/>), which permits unrestricted use, distribution, and reproduction in any medium, provided you give appropriate credit to the original author(s) and the source, provide a link to the Creative Commons license, and indicate if changes were made.

References

- Antoni, M., Rossen, J., Martirena, F., & Scrivener, K. (2012). Cement substitution by a combination of metakaolin and

- limestone. *Cement and Concrete Research*, 42(12), 1579–1589.
- Aqel, M., & Panesar, D. K. (2016). Hydration kinetic and compressive strength of steam-cured cement pastes and mortars containing limestone filler. *Construction and Building Materials*, 113(1), 359–368.
- Bentz, D. P. (2006). Modeling the influence of limestone filler on cement hydration using CEMHYD3D. *Cement & Concrete Composites*, 28(2), 124–129.
- Bonavetti, V., Donza, H., Menendez, G., Cabrera, O., & Irassar, E. F. (2003). Limestone filler cement in low w/c concrete: A rational use of energy. *Cement and Concrete Research*, 33(6), 865–871.
- Carrasco, M. F., Menendez, G., Bonavetti, V., & Irassar, E. F. (2005). Strength optimization of tailor-made cement with limestone filler and blast furnace slag. *Cement and Concrete Research*, 35(7), 1324–1331.
- Gao, Y., De Schutter, G., Ye, G., Yu, Z., Tan, Z., & Wu, K. (2013). A microscopic study on ternary blended cement based composites. *Construction and Building Materials*, 46(1), 28–38.
- Ghrici, M., Kenai, S., & Said-Mansour, M. (2007). Mechanical properties and durability of mortar and concrete containing natural pozzolana and limestone blended cements. *Cement & Concrete Composites*, 29(7), 542–549.
- Hoshino, S., Yamada, K., & Hirao, H. (2006). XRD/rietveld analysis of the hydration and strength development of slag and limestone blended cement. *Journal of Advanced Concrete Technology*, 4(3), 357–367.
- Ipavec, A., Gabrovsek, R., Vuk, T., Kaucic, V., Macek, J., & Meden, A. (2011). Carboaluminate phases formation during the hydration of calcite-containing portland cement. *Journal of American Ceramic Society*, 94(4), 1238–1242.
- Lee, H. S., & Wang, X. Y. (2016). Evaluation of compressive strength development and carbonation depth of high volume slag-blended concrete. *Construction and Building Materials*, 124(1), 45–54.
- Lothenbach, B., Saout, G. L., Gallucci, E., & Scrivener, K. (2008). Influence of limestone on the hydration of Portland cements. *Cement and Concrete Research*, 38(6), 848–860.
- Maekawa, K., Ishida, T., & Kishi, T. (2009). *Multi-scale modeling of structural concrete*. London: Taylor & Francis.
- Menendez, G., Bonavetti, V., & Irassar, E. F. (2003). Strength development of ternary blended cement with limestone filler and blast-furnace slag. *Cement & Concrete Composites*, 25(1), 61–67.
- Mounanga, P., Khokhar, M. I. A., Hachem, R. E., & Loukili, A. (2011). Improvement of the early-age reactivity of fly ash and blast furnace slag cementitious systems using limestone filler. *Materials and Structures*, 44(2), 437–453.
- Papadakis, V. G. (2000). Effect of supplementary cementing materials on concrete resistance against carbonation and chloride ingress. *Cement and Concrete Research*, 30(2), 291–299.
- Wang, X. Y. (2017). Modeling of hydration, compressive strength, and carbonation of portland-limestone cement (PLC) concrete. *Materials*, 10(1), 115–131.
- Weerd, K. D., Ben Haha, M., Saout, G. L., Kjellsen, K. O., Justnes, H., & Lothenbach, B. (2011). Hydration mechanisms of ternary Portland cements containing limestone powder and fly ash. *Cement and Concrete Research*, 41(3), 279–291.